Published in final edited form as:
Circ Res. 2008 December 5; 103(12): 1483–1491. doi:10.1161/CIRCRESAHA.108.177055.

Homozygous Missense N629D hERG (KCNH2) Potassium Channel Mutation Causes Developmental Defects in the Right Ventricle and its Outflow Tract and Embryonic Lethality

Guo Qi Teng, **Xian Zhao**, **James P. Lees-Miller**, **F. Russell Quinn**, **Pin Li**, **Derrick E. Rancourt**, **Barry London**, **James C. Cross**, and **Henry J. Duff**
Libin Cardiovascular Institute, Faculty of Medicine, Department of Comparative Biology & Experimental Medicine, Faculty of Veterinary Medicine, University of Calgary, Canada and Cardiovascular Institute University of Pittsburgh

Abstract

Loss-of-function mutations in the human ERG1 potassium channel (hERG1) frequently underlie the Long QT2 Syndrome. The role of the ERG potassium channel in cardiac development was elaborated in an *in vivo* model of a homozygous, loss of function, LQT2 Syndrome mutation. The hERG N629D mutation was introduced into the orthologous mouse gene, mERG, by homologous recombination in mouse embryonic stem cells. Intact homozygous embryos showed abrupt cessation of the heart beat. N629D/N629D embryos die *in utero* by E11.5. Their developmental defects include: altered looping architecture; poorly developed bulbus cordis; distorted aortic sac and branchial arches. N629D/N629D myocytes from E9.5 embryos manifested complete loss of IKr function, depolarized resting potential, prolonged action potential duration (LQT), failure to repolarize and propensity to oscillatory arrhythmias. N629D/N629D myocytes manifest calcium oscillations and increased SR Ca^{+2} – content. While the N629D/N629D protein is synthesized it is mainly located intracellularly; whereas +/+ mERG protein is mainly in plasmalemma. N629D/N629D embryos show robust apoptosis in cranio-facial regions, particularly in the first branchial arch and to a lesser extent in the cardiac outflow tract. Since deletion of Hand2 produces apoptosis, in similar regions and with a similar final developmental phenotype, Hand2 expression was evaluated. Robust decrease in Hand2 expression was observed in the secondary heart field in N629D/N629D embryos. In conclusion, loss of IKr function in N629D/N629D cardiovascular system leads to defects in cardiac ontogeny in the first branchial arch, outflow tract and the right ventricle.

Keywords

KCNH2(hERG); knock-in-mouse; embryo developmental defect

INTRODUCTION

The human *ERG* gene (*hERG/KCNH2*) encodes a potassium channel that is important in the late stage of action potential repolarization in heart. Mutations in this gene, which generally reduce plasma-lemmal expression of hERG, lead to the Long QT2 Syndrome in humans [1–2]. Patients with the Long QT Syndrome have a delay in cardiac repolarization which

Address for Correspondence: Henry J. Duff, M.D, Libin Cardiovascular Institute, University of Calgary, 3330 Hospital Drive, N.W., Calgary, Canada, T2N 4N1, Telephone: (403) 220-4525, Fax: (403) 270-0313.
The first two authors contributed equally to this work.

Disclosures: None.

predisposes them to cardiac arrhythmias that can be lethal [1,2]. Mutations in hERG are associated with embryonic lethality and the sudden infant death syndrome [3–4]. While the LQT2 Syndrome generally occurs in individuals heterozygous for the mutant allele, individuals homozygous for the exon 4 duplication manifest embryonic lethality or are rescued in the neonatal period by pacing [5]. Although not widely recognized, mutations of hERG appear to be associated with structural congenital cardiovascular anomalies including: Tetralogy of Fallot, atrial-septal defects, ventricular-septal defects and patent ductus arteriosus [6–9]. Mouse ERG (mERG) is the dominant repolarizing current in the mouse embryonic heart [10]. A channel analogous to hERG is expressed in differentiating quail neural crest cells [11] early in development. These data imply a potential role of the ERG potassium channel in cardiovascular development. We created, by homologous recombination in embryonic mouse stem cells, mice bearing the human LQT2 N629D hERG mutation [12–16] inserted *in situ* in the mouse gene homologue (mERG). The cardiovascular developmental consequences were evaluated.

METHODS

The methods used to create the N629D mice are detailed in the Online Supplement. All animals were housed in the Animal Resource Centre of the Faculty of Medicine, University of Calgary, Alberta, Canada, using protocols in accordance with animal care guidelines established by the Canadian Council on Animal Care.

Immunohistochemistry and immunofluorescence

For Immunohistochemistry, cryo-section was made from 4% PFA fixed embryos, sections were cut at 10 μm, and incubated in blocking solution (PBS containing 0.1 % Triton X-100, 0.05% Tween20, 2 % donkey serum and 1% BSA) for 2 h, followed by overnight incubation in the anti-HERG antibodies 1:300, (Alomone labs, Israel) in 1% BSA PBS solution at 4o C. As negative control, 10 μg/ml of the mERG peptide was added together with the first antibody. After washing, sections were incubated in blocking solution 2 hours, then incubated with donkey anti-rabbit HRP conjugate (Amersham) 1:300. For immunoflourescence, cardiomyocytes or cryo-sections from OCT embedded embryos were fixed with −20°C methanol for 10 minutes, and then blocked and labeled with mERG antibody as described above followed by incubation with cy3 conjugated goat anti-rabbit secondary antibody (Jackson Immunoresearch Laboratories, West Grove, PA).

In situ hybridization

Whole mount in situ hybridization was performed on E9.5 +/+ and N629D/N629D embryos [17]. An EcoR1/Xho1 fragment at the 3' end of the coding sequence was subcloned into pGEN-T easy vector to produce the mERG1 specific probe [18]. The Hand2 probe consisted of a 1.2kb fragment from the 3' end of Hand2 cDNA.[19]. *In situ* hybridization studies were also performed with a mERG1 probe.

Apoptosis assay

TUNEL assays were carried out using Chemicon's Apoptag Peroxidase In Situ Apoptosis Detection Kit.

Isolated Murine Embryonic Cardiomyocytes and Electrophysiological Recording

Isolation and dispersion of E9.5 cardiomyocytes were performed by the method similar to that described by Burton [20]. The extracellular solution (36 ± 1 °C) contained 140 mM NaCl, 5.4 mM KCl, 1 mM $MgCl_2$, 1 mM $CaCl_2$, 5 mM HEPES, 5.5 mM glucose, (pH 7.4 with NaOH). The pipette solution contained 110 mM K-aspartate, 10 mM KCl, 5 mM MgCl2, 5 mM ATP-

Na_2, 10 mM EGTA, 10 mM HEPES, and 1 mM $CaCl_2$ (pH 7.2 with KOH). A liquid junction potential of – 10 mV was corrected. The holding potential was −70 mV.

Intracellular calcium measurement

Cells were loaded with the membrane-permeable acetoxymethyl ester of Fluo-4 (Fluo-4-AM, Molecular Probes, Invitrogen Inc.) and intracellular Ca^{2+} transients were measured at 37°C (see Methods Supplement). Membrane potential was simultaneously measured in current-clamp mode. Sarcoplasmic reticulum (SR) Ca^{2+} content was estimated from the amplitude of the Ca^{2+} transient induced by rapid application of 10 mM caffeine.

Video Microscopy

Pregnant females at 9.5 dpc (days post coutis) were anesthetized (isoflurane) and the embryos placed in DMEM at 37 ° C. Video microscopy was performed at 10-power using a digital video camera.

In vivo Embryonic Echocardiography

An echocardiographic machine (Model VS40; VisualSonics, nominal center frequency of 40 MHz and a focal length of 6 mm Toronto, Canada) was used [21] to observe the characteristics of the intrauterine heart beating.

RESULTS

Homozygous N629D Results in Embryonic Lethality

The N629D mutation was inserted into the mouse ERG gene by homologous recombination in mouse embryonic stem cells (see Online Figure I). To remove the neomycin cassette, N629D mice were mated to Mox2-Cre mice.

Heterozygous N629D mutant offspring were viable and fertile. However, no viable N629D/N629D homozygous offspring were obtained in litters from N629D heterozygote intercrosses (Online Figure I B). To further explore when N629D/N629D embryos die, embryos were dissected at various times during gestation. Their genotypes and morphologies were related (Figure 1 and Online Figure I). Before E9.0 no obvious difference in body size at matched stages of development (as judge by somite pairs) was observed (Figure 1 Panel A and H). After 20 somites, the N629D/N629D embryos showed significantly smaller body size. By E11.5 no live N629D/N629D embryos were found.

Developmental Cardiac Defects in N629D/N629D Embryos

At E9.5, the morphology of the +/+ hearts shows the expected bulboventricular groove and a U-shaped cardiac loop (Figure 1, Panel B, see arrow). In contrast, the N629D/N629D embryos (Panel I) did not show this normal bulboventricular groove (n = 14) and instead the silhouette of the heart showed an L-shaped heart tube. These data suggested abnormalities in looping architecture. N629D/N629D embryos were observed to have a massive pericardial effusion; likely a consequence of heart failure. Defective development was observed in the bulbus cordis right ventricle and the outflow tract. Figure 1 (C, D, E) compares representative H&E coronal sections of the embryos at E9.5 in +/+ versus N629D/N629D embryos (Panel J, K, L). In N629D/N629D embryos, the right ventricle is not normally developed; the outflow tract is distorted and is continuous with a dilated aortic sac and first branchial arch artery. Hypoplasia of first branchial arch is shown in Figure 1, Panel J. Heterozygote embryos have neither developmental phenotypes nor pericardial effusion.

To assess whether the N629D/N629D genotype altered the overall expression levels of wild type or mutant mERG protein, immunohistology studies were done in +/+ Figure 1 Panels F, Panel G (higher power magnification of boxed portion of Panel F) and in N629D/N629D hearts Panels M and N (higher power). Overall mERG protein expression is similar in +/+ (Panels F,G) and N629D/N629D hearts (Panels M,N).

The +/+ hearts consistently beat regularly without arrhythmias. In contrast, N629D/N629D hearts beat irregularly with abrupt pauses (attached video supplement). The +/+ embryos shows flow both into and out of the heart. The N629D/N629D embryos have arrhythmias and there is no flow into or out of the heart even during normal beats. Fetal echocardiograms confirm irregular beating and abrupt asystolic episodes in N629D/N629D mice, but never in +/+ embryos.

I_{Kr}, Action Potential and Arrhythmic Phenotypes in N629D/N629D Myocytes

At E9.5, WT myocytes show typical hERG currents (Figure 2, Panel A), whereas complete loss of I_{Kr} tail-current was observed in the N629D/N629D myocytes (Panel B). While most of the +/N629D myocytes from 10 hearts (29/38) have an I_{Kr} whose character and density is similar to +/+ (Panel C), a minority of myocytes (6/38) showed an I_{Kr} with a much smaller ratio of tail current to time-dependent current magnitude (Panel D). This characteristic is the same as the “intermediate” phenotype previously reported [13–15]. In addition, a small proportion of +/N629D cells (3/38) showed an N629D-like phenotype; absent tail-currents (Panel E). Mean current-voltage relationships of the peak tail-currents are shown in Figure 2, Panel F.

For each and every cell, after recording I_{Kr} in voltage-clamp mode, spontaneous paired action potentials were recorded in current-clamp mode. In +/+ myocytes, a spectrum of action potential shapes were observed; some with features of sinus node cells, some atrial-like and some ventricular-like (Figure 3, Panel A). Even so, +/+ myocytes manifest relatively hyperpolarized resting membrane potentials (mean data in Online Figure II). In comparison to +/+, the action potential in N629D/N629D myocytes (Figure 3, Panel B) show more depolarized resting membrane potentials and prolonged action potential durations. Moreover, failure to repolarize and spontaneous oscillatory triggered activity were commonly observed in N629D/N629D myocytes (Figure 3 Panel B). Most +/N629D cells had a wild type-like I_{Kr} phenotype (Panel C) and had action potentials similar to +/+. In contrast, +/N629D myocytes which manifest the “intermediate” I_{Kr} phenotype (Panel D) had resting potentials that were significantly more depolarized with prolonged action potentials. In addition, cells with an N629D-like phenotype had marked depolarization of resting potential and spontaneous arrhythmias occurred frequently (Figure 3 Panel E). The +/+ myocytes manifest a resting membrane potential of -64 ± 2 mV compared to -38 ± 2 mV for N629D/N629D myocytes ($p<0.001$). The +/N629D cells with a wild type-like I_{Kr} phenotype (Panel C) had a resting potential (-67 ± 1 mV) similar to +/+. In contrast, +/N629D myocytes which manifest the “intermediate” and N629D-like I_{Kr} phenotype (Panel D) had depolarized resting potentials of -50 ± 4 mV and -39 ± 3 mV respectively; both $p<0.01$). Mean action potential durations (in msec) for +/+, N629D/N629D, +/N629D with wild type-like phenotype, +/N629D-intermediate I_{Kr} phenotype, and +/N629D- N629D-like phenotypes were 65± 6; 143± 25 $p<0.01$; 59± 12 (NS); 139± 30 $P<0.01$;145± 29 msec $p<0.01$, respectively.

Distribution of N629D Protein Expression in Myocytes

To assess the cellular distribution of the N629D protein, immunocytochemical studies were performed on cardiac myocytes isolated from E9.5 heart tubes. The distributions of the mERG protein are shown in Figure 3 in the right hand column. Typically the +/+ mERG protein is localized dominantly in the surface plasma-lemma where it is expressed as continuous linear

sheaths of staining. In contrast, the N629D/N629D protein was expressed intracellular, in a pattern of punctuate concentric rings of staining which do not generally touch the plasma-lemma. In contrast, a spectrum of expression patterns are observed in heterozygous +/N629D myocytes. The majority of the cells (108/133 cells) had a pattern of distribution of mERG protein similar to WT. A minority of cells (14/ 133 cells) had a pattern of staining indistinquishable from N629D/N629D myocytes. The remaining cells had an intermediate pattern, wherein the mERG protein was expressed in punctuate dots in a subplasma-lemmal location, with some expression likely in the plasma-lemma as well. The proportions of +/N629D cells showing a WT-like phenotype by electrophysiology (29/38 cells; 76% of cells) were roughly equivalent to the proportion of cells showing a WT-like phenotype on immunocytochemistry (108/133; 81%). The same is true in terms of the proportions of cells showing intermediate and N629D-like electrophysiology and immunocytochemical phenotype. Lower power images of the cellular distribution of mERG proteins are shown in Online Figure III.

N629D/N629D myocytes manifest calcium oscillations and increased SR Ca^{+2}–content

Since involution of the fetus and failure of the heart to develop are characteristics of the N629D/N629D embryos and since abnormalities of intracellular calcium are a common denominator of cell death [22] we compared intracellular calcium homeostasis in N629D/N629D versus +/+ E9.5 fetal myocytes (Figure 4). The N629D/N629D cells were depolarized and they displayed abnormal Ca^{2+} oscillations, with elevated peak F/F_0 (Fig.4, A, B). In these circumstances, injection of negative current (to give a resting membrane potential comparable to that of WT cells) lowered diastolic F/F_0 and produced abnormal prolonged action potentials with marked early afterdepolarizations (Fig. 4, A.B). The SR-Ca^{2+} content (estimated from the amplitude of the caffeine-induced Ca^{2+} transient) was significantly higher in N629D cells (F/F_0: N629D 4.02±0.24, versus WT 3.40±0.17, p=0.04, Fig.4,C.D).

Potential Mechanisms by Which mERG K^+ Channel Plays a Role in Development

mERG expression was abundant in the cranio-facial region and first branchial arch (Figure 5 Panel A). mERG expression was also compared in right ventricle, outflow tract and left ventricle in +/+ embryos. The expression of mERG protein was substantially stronger in the right ventricle and outflow tract compared to the left ventricle in +/+ E10.5 embryonic heart (Figure 5 Panel B). Since the developmental defects seen in the N629D/N629D fetuses are quite similar to that seen in *Hand2* deficient embryos [23] we assessed Hand2 expression in the N629D/N629D embryonic hearts versus +/+. Figure 6 shows that in +/+ embryos *Hand2* is abundantly expressed in the right ventricle, bulbus cordis and the branchial arches, compared to the left ventricle. In contrast, Hand2 is substantially down-regulated in N629D/N629D E9.5 embryos (Figure 6).

Apoptosis is also seen in the first branchial arch in hand2-deleted mice at E9.5 [23]. TUNEL immunocytochemical assays were also performed on N629D/N629D embryos. Figure 7 shows robust TUNEL-positive staining at E9.5 in N629D/N629D fetuses in the cranio-facial region. Apoptotic cells were also observed in the outflow tract of the N629D/N629D hearts, albeit sporadically, but were rare in these areas in the +/+ embryos. Our data indicates that the earliest signs of apoptosis develop in the first branchial arches (Figure 1, Panel J and Figure 7 Panel C) and cranial-facial regions. To assess the time-course of the onset of the apoptosis we assessed the presence of apoptosis at earlier developmental times. Even earlier, at E9 (somite 17–19) robust apoptosis was present in the cranial-facial maxillary regions and the first branchial arches in N629D/N629D embryos. At that time there was no witnessed apoptosis in the heart (data not shown). No overt difference in phospho-histone H3 staining (M- phase marker) was observed comparing E9.5 N629D/N629D and +/+ embryos (data not shown).

DISCUSSION

The N629D/N629D embryos show the following novel features: 1) all embryos die by E11.5; 2) an I_{Kr}-null phenotype is associated with defects in cardiac looping and development of the right ventricle, bulbus cordis and pharyngeal arches. These gross histopathologic phenotypes are very similar to that reported in abstract form by London et al [24]. 3) N629D/N629D myocytes show prolonged APD and depolarization of the resting potential and propensity to oscillatory cardiac arrhythmias and recurrent asystolic episodes in intact embryos. 4) The depolarization of the resting potential is associated with abnormalities of intracellular calcium homeostasis. Intracellular calcium overload is a common denominator to cell death in excitable tissues [22]. 5) Apoptosis is abundant at E 9.5 in the cranio-facial region and the first branchial arch and this occurs before apoptosis in the outflow tract.

Since a large number of medications inadvertently block the hERG potassium channel, these novel findings have substantial clinical relevance.

Causes of Embryonic Lethality

There are a number of reasons to believe that the cardiovascular defects are causative of the embryonic lethality: a) all propulsive flow into and out of the fetal heart is lost in the N629D/N629D embryos; b) embryonic N629D/N629D embryos manifest arrhythmias and bradycardias. Previous studies report that embryonic hearts respond to pharmacological hERG blockers with bradycardia and cardiac arrest resulting in ischemia [25–28], ventriculo-septal defects, vascular defects and death. One limitation of those studies is that the drugs used are not at all specific for I_{Kr}. Secondly, blockade of I_{Kr} in embryonic cardiac myocytes was not established.

Potential Mechanisms by Which mERG K^+ Channel Plays a Role in Development

In the present study, we observed that mERG protein expression in the developing embryonic heart is not homogeneous. Protein expression is exaggerated in the right ventricle and in the outflow tract. Previous studies by Franco [29] also reported inhomogeneous expression of beta subunits of the I_{Kr} channel complex in embryonic heart: expression mIRP and minK are also exaggerated in the bulbus cordis[29]. An exaggerated phenotype of the functionally knock-out might be expected in tissue with endogenous exaggerated mERG expression.

Recent studies in chicken embryos by Tirosh-Finkel et al [30] indicate that cells from the cranial paraxial mesoderm migrate to the branchial arches and subsequently give rise to the facial structures and populate the outflow tract of the heart. Other studies by Ko et al [31] propose that cranial neural crest cells appear to contribute to cardiac outflow tract. N629D/N629D embryos manifest extensive apoptosis particularly in the first branchial arch and the facial region. Given that cells from the branchial arch populate the outflow tract [30], we propose that early apoptosis, in the branchial arch and facial region would prevent those cells from contributing to the development of the outflow tract in N629D/N629D hearts [30,31]. This is our working model. Thus we propose that Hand2 expression is down regulated in N629D/N629D embryonic right ventricle and outflow tract because progenitor cells that populate the outflow tract undergo apoptosis while in the facial region and branchial arch. Thus tissues that would be expected to express Hand2 are absent, simply because those structures fail to develop.

Previous studies indicate that Hand2 deletion results in cranio-facial apoptosis with defects in the development of the right ventricle, outflow tract and bulbus cord. Thus, deletion of *Hand2* produces a final developmental phenotype [32] similar to N629D/N629D embryos. The molecular mechanism underlying the defect in the pharyngeal arches in *Hand2* null mice has

been recently explored showing apoptosis in an Apaf-1-dependent fashion, Apaf-1 is a central downstream mediator of mitochondrial damage-induced apoptosis[33].

Our data indicates the deficiency of mERG functional expression in N629D/N629D embryos results in depolarization of the resting membrane potential. We propose a working mechanistic model in which protracted depolarization of the resting membrane potential triggers apoptosis due to intracellular calcium overload. Dysfunction of calcium homeostasis is a common trigger for apoptosis in a wide range of cellular systems, including heart [22]. Other studies confirm that pharmacologic block of hERG results in apoptosis. The antihypertensive agent, doxazosin pharmacologically blocks the hERG channel [34]. Specifically doxazosin induced apoptosis in hERG-overexpressing HEK cells, but did not produce apoptosis in untransfected control cells. Pharmacologic blockade of hERG also leads to apoptosis in wide range of native tumor cells that endogenously over-express the hERG current[35].

An alternative working model for the apoptosis and mortality in N629D/N629D mice is that the proven arrhythmias and asystolic episodes and abnormalities of flow lead to hemodynamic insufficiency which can secondarily increase apoptosis, change Ca2+ handling and induce heart defects. Evenso, this does not readily explain why the apoptosis begins in the branchial arch.

Limitations

Our study provides a working hypotheses to explain the developmental defects in N629D/N629D mice. While our model is based on and is consistent with our data, we can not unambiguously prove that all of the phenotypes observed in N629D/N629D embryos are caused by a loss of function of I_{Kr}, subsequent depolarization-mediated calcium overload resulting in apoptosis. It remains a possibility that the N629D mutation results in a “gain of function” in non-cardiac cells. Further studies will be necessary to address these issues.

In conclusion, loss of IKr function in the N629D/N629D cardiovascular system leads to defects in cardiac ontogeny mainly in the first branchial arch, outflow tract and the right ventricle.

Supplementary Material

Refer to Web version on PubMed Central for supplementary material.

Acknowledgments

Sources of Funding

This work was funded by the Alberta heart and Stroke Foundation, and the Canadian Institutes of Health Research; Dr. Duff receives personnel funding from the Alberta Heritage Foundation of Medical Research.

CIHR - Operating Grant - 2007–2012

Canadian Institutes of Health Research; Mutant mERG Channels in Embryonic

Growth/Development in the Adult Mouse

HSFA Grant-in-aid - 2007 – 2009

Heart and Stroke Foundation of Alberta; Endowed Chair in Cardiovascular Medicine

Medical Scientist for the Alberta Heritage Foundation for Medical Research 1992 – Present

Grant acknowledgements for Barry London

AHA Established Investigator Award 0540048N and NIH R01 HL58030

REFERENCES

1. Roden DM, Spooner PM. Inherited long QT syndromes: a paradigm for understanding arrhythmogenesis. J Cardiovasc Electrophysiol 1999;10:1664–1683. [PubMed: 10636197]
2. Towbin JA, Wang Z, Li H. Genotype and severity of long QT syndrome. Arch Pathol Lab Med 2001;125:116–121. [PubMed: 11151064]
3. Christiansen M, Tønder N, Larsen LA, Andersen PS, Simonsen H, Oyen N, Kanters JK, Jacobsen JR, Fosdal I, Wettrell G, Kjeldsen K. Mutations in the HERG K+-ion channel: a novel link between long QT syndrome and sudden infant death syndrome. Am J Cardiol 2005;95:433–434. [PubMed: 15670565]
4. Antzelevitch C. Molecular biology and cellular mechanisms of Brugada and long QT syndromes in infants and young children. J Electrocardiol 2001;34:177–181. [PubMed: 11781953]
5. Hoorntje T, Alders M, van Tintelen P, van der Lip K, Sreeram N, van der Wal A, Mannens M, Wilde A. Homozygous premature truncation of the HERG protein: the human HERG knockout. Circulation 1999;100:1264–1267. [PubMed: 10491368]
6. Stéphan E, Ashoush R, Mégarbané A, Kassab R, Salem N, Loiselet J, Bouvagnet P. [Autosomal dominant Mendelian midline complex. Secundum atrial septal defect associated with cardiac and facial-thoracic defects. A familial case]. Arch Mal Coeur Vaiss 2000;93:641–647. [PubMed: 10858865]
7. Wu MH, Hsieh FC, Wang JK, Kau ML. A variant of long QT syndrome manifested as fetal tachycardia and associated with ventricular septal defect. Heart 1999;82:386–388. [PubMed: 10455095]
8. Walls J, Sanatani S, Hamilton R. Post-hoc diagnosis of congenital long QT syndrome in patients with tetralogy of Fallot. Pediatr Cardiol 2005;26:107–110. [PubMed: 15793661]
9. Murugan SJ, Parsons JM, Bennett C. A case of long QT syndrome associated with familial occurrence of persistent patency of the arterial duct. Cardiol Young 2005;15:309–311. [PubMed: 15865837]
10. Wang L, Feng ZP, Kondo CS, Sheldon RS, Duff HJ. Developmental changes in the delayed rectifier K+ channels in mouse heart. Circ Res 1996;79:79–85. [PubMed: 8925572]
11. Arcangeli A, Rosati B, Cherubini A, Crociani O, Fontana L, Ziller C, Wanke E, Olivotto M. HERG- and IRK-like inward rectifier currents are sequentially expressed during neuronal development of neural crest cells and their derivatives. Eur J Neurosci 1997;9:2596–2604. [PubMed: 9517465]
12. Satler CA, Vesely MR, Duggal P, Ginsburg GS, Beggs AH. Multiple different missense mutations in the pore region of HERG in patients with long QT syndrome. Hum Genet 1998;102:265–272. [PubMed: 9544837]
13. Lees-Miller JP, Duan Y, Teng GQ, Thorstad K, Duff HJ. Novel gain-of-function mechanism in K(+) channel-related long-QT syndrome: altered gating and selectivity in the HERG1 N629D mutant. Circ Res 2000;86:507–513. [PubMed: 10720411]
14. Teng GQ, Lees-Miller JP, Duan Y, Li BT, Li P, Duff HJ. [K(+)](o)-dependent change in conformation of the HERG1 long QT mutation N629D channel results in partial reversal of the in vitro disease phenotype. Cardiovasc Res 2003;57:642–650. [PubMed: 12618226]
15. Teng G, Zhao X, Cross JC, Li P, Lees-Miller JP, Guo J, Dyck JR, Duff HJ. Prolonged repolarization and triggered activity induced by adenoviral expression of HERG N629D in cardiomyocytes derived from stem cells. Cardiovasc Res 2004;61:268–277. [PubMed: 14736543]
16. Gong Q, Anderson CL, January CT, Zhou Z. Role of glycosylation in cell surface expression and stability of HERG potassium channels. Am J Physiol Heart Circ Physiol 2002;283:H77–H84. [PubMed: 12063277]
17. Conlon RA, Rossant J. Exogenous retinoic acid rapidly induces anterior ectopic expression of murine Hox-2 genes in vivo. Development 1992;116:357–368. [PubMed: 1363087]
18. London B, Trudeau MC, Newton KP, Beyer AK, Copeland NG, Gilbert DJ, Jenkins NA, Satler CA, Robertson GA. Two isoforms of the mouse ether-a-go-go-related gene coassemble to form channels with properties similar to the rapidly activating component of the cardiac delayed rectifier K+ current. Circ Res 1997;81:870–878. [PubMed: 9351462]
19. Cross JC, Flannery ML, Blanar MA, Steingrimsson E, Jenkins NA, Copeland NG, Rutter WJ, Werb Z. Hxt encodes a basic helix-loop-helix transcription factor that regulates trophoblast cell development. Development 1995;121:2513–2523. [PubMed: 7671815]

20. Burton PB, Raff MC, Kerr P, Yacoub MH, Barton PJ. An intrinsic timer that controls cell-cycle withdrawal in cultured cardiac myocytes. Dev Biol 1999;216:659–670. [PubMed: 10642800]
21. Zhou YQ, Foster FS, Qu DW, Zhang M, Harasiewicz KA, Adamson SL. Applications for multifrequency ultrasound biomicroscopy in mice from implantation to adulthood. Physiol Genomics 2002;10:113–126. [PubMed: 12181368]
22. Chen X, Zhang X, Kubo H, Harris DM, Mills GD, Moyer J, Berretta R, Potts ST, Marsh JD, Houser SR. Ca2+ influx-induced sarcoplasmic reticulum Ca2+ overload causes mitochondrial-dependent apoptosis in ventricular myocytes. Circ Res 2005;97:1009–1017. [PubMed: 16210547]
23. Thomas T, Kurihara H, Yamagishi H, Kurihara Y, Yazaki Y, Olson EN, Srivastava D. A signaling cascade involving endothelin-1, dHAND and msx1 regulates development of neural-crest-derived branchial arch mesenchyme. Development 1998;125:3005–3014. [PubMed: 9671575]
24. London B. Qt interval Prolongation and Arrhythmias in Heterozygous Merg1-Targeted Mice. Circulation 1998:279.
25. Danielsson C, Azarbayjani F, Sköld AC, Sjögren N, Danielsson BR. Polytherapy with hERG-blocking antiepileptic drugs: increased risk for embryonic cardiac arrhythmia and teratogenicity. Birth Defects Res. A Clin Mol Teratol 2007;79:595–603. [PubMed: 17584909]
26. Sköld AC, Danielsson BR. Developmental toxicity in the pregnant rabbit by the class III antiarrhythmic drug sotalol. Pharmacol Toxicol 2001;88:34–39. [PubMed: 11169159]
27. Danielsson BR, Skold AC, Azarbayjani F. Class III antiarrhythmics and phenytoin: teratogenicity due to embryonic cardiac dysrhythmia and reoxygenation damage. Curr Pharm Des 2001;7:787–802. [PubMed: 11375779]
28. Wellfelt K, Sköld AC, Wallin A, Danielsson BR. Teratogenicity of the class III antiarrhythmic drug almokalant. Role of hypoxia and reactive oxygen species. Reprod Toxicol 1999;13:93–101. [PubMed: 10213516]
29. Franco D, Demolombe S, Kupershmidt S, Dumaine R, Dominguez JN, Roden D, Antzelevitch C, Escande D, Moorman AF. Divergent expression of delayed rectifier K(+) channel subunits during mouse heart development. Cardiovasc Res 2001;52:65–75. [PubMed: 11557234]
30. Tirosh-Finkel L, Elhanany H, Rinon A, Tzahor E. Mesoderm progenitor cells of common origin contribute to the head musculature and the cardiac outflow tract. Development 2006;133:1943–1953. [PubMed: 16624859]
31. Ko SO, Chung IH, Xu X, Oka S, Zhao H, Cho ES, Deng C, Chai Y. Smad4 is required to regulate the fate of cranial neural crest cells. Dev Biol 2007;312:435–447. [PubMed: 17964566]
32. Srivastava D, Thomas T, Lin Q, Kirby ML, Brown D, Olson EN. Regulation of cardiac mesodermal and neural crest development by the bHLH transcription factor, dHAND. Nat Genet 1997;16:154–160. [PubMed: 9171826]
33. Aiyer AR, Honarpour N, Herz J, Srivastava D. Loss of Apaf-1 leads to partial rescue of the HAND2-null phenotype. Dev Biol 2005;278:155–162. [PubMed: 15649468]
34. Thomas D, Bloehs R, Koschny R, Ficker E, Sykora J, Kiehn J, Schlömer K, Gierten J, Kathöfer S, Zitron E, Scholz EP, Kiesecker C, Katus HA, Karle CA. Doxazosin induces apoptosis of cells expressing hERG K+ channels. Eur J Pharmacol 2008;579:98–103. [PubMed: 18054910]
35. Shao XD, Wu KC, Guo XZ, Xie MJ, Zhang J, Fan DM. Expression and significance of HERG protein in gastric cancer. Cancer Biol Ther 2008;7:45–50. [PubMed: 17938585]

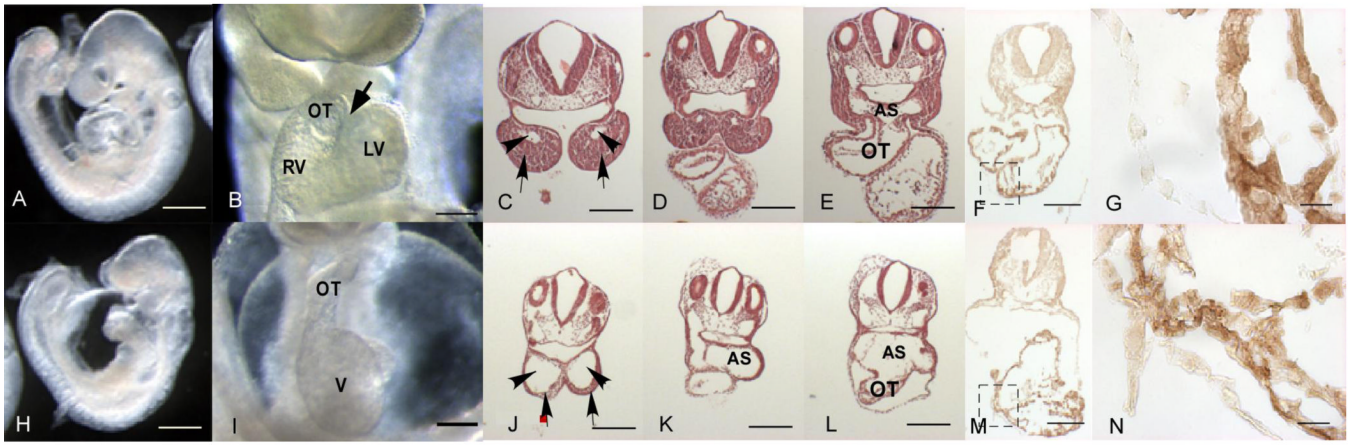

Figure 1. Overall embryonic growth characteristics and assessment of cardiac defects in N629D mutant embryos

Top row shows +/+ and the bottom row shows N629D/N629D embryos. Panel A shows the embryonic size of +/+ embryos versus homozygous N629D /N629D in Panels (H) at E 9.0. Panel B shows the ventral views of E9.5 +/+ versus homozygous N629D/N629D hearts in Panel I. Normal looping with bulboventricular groove (arrow) and a U- shaped cardiac loop in wild type (B) whereas pericardial effusion and overall defective looping and abnormal cardiac morphological architecture including poor development of the proximal parts of the outflow tract were found in homozygous N629D/N629D embryos (I). LV indicates left ventricle, RV indicates right ventricle and OT indicates outflow tract. In the homozygous N629D mice it is difficult to distinguish right and left ventricles and primitive ventricle is labeled V. Panel C,D,E show the hematoxylin and eosin stained coronal sections of +/+ embryos versus the homozygous N629D/N629D embryos (J,K,L). The N629D/N629D embryos show a poorly developed bulbus cordis. The first branchial arch and aortic sac are dilated and distorted. Arrowhead in C and J show 1st branchial arch artery and arrow shows the mandible; AS, aortic sac; OT, outflow track. The bars in Panels G, N indicate 20 μM, in other panels = 200 μM.

Panel F, M (lower power) and G, N (higher power magnification of boxed regions of F,M) show overall immunohistochemical protein expression in +/+ (F, G) versus N629D/N629D hearts (M, N). Overall N629D/N629D protein expression is not substantially reduced compared to +/+ protein expression.

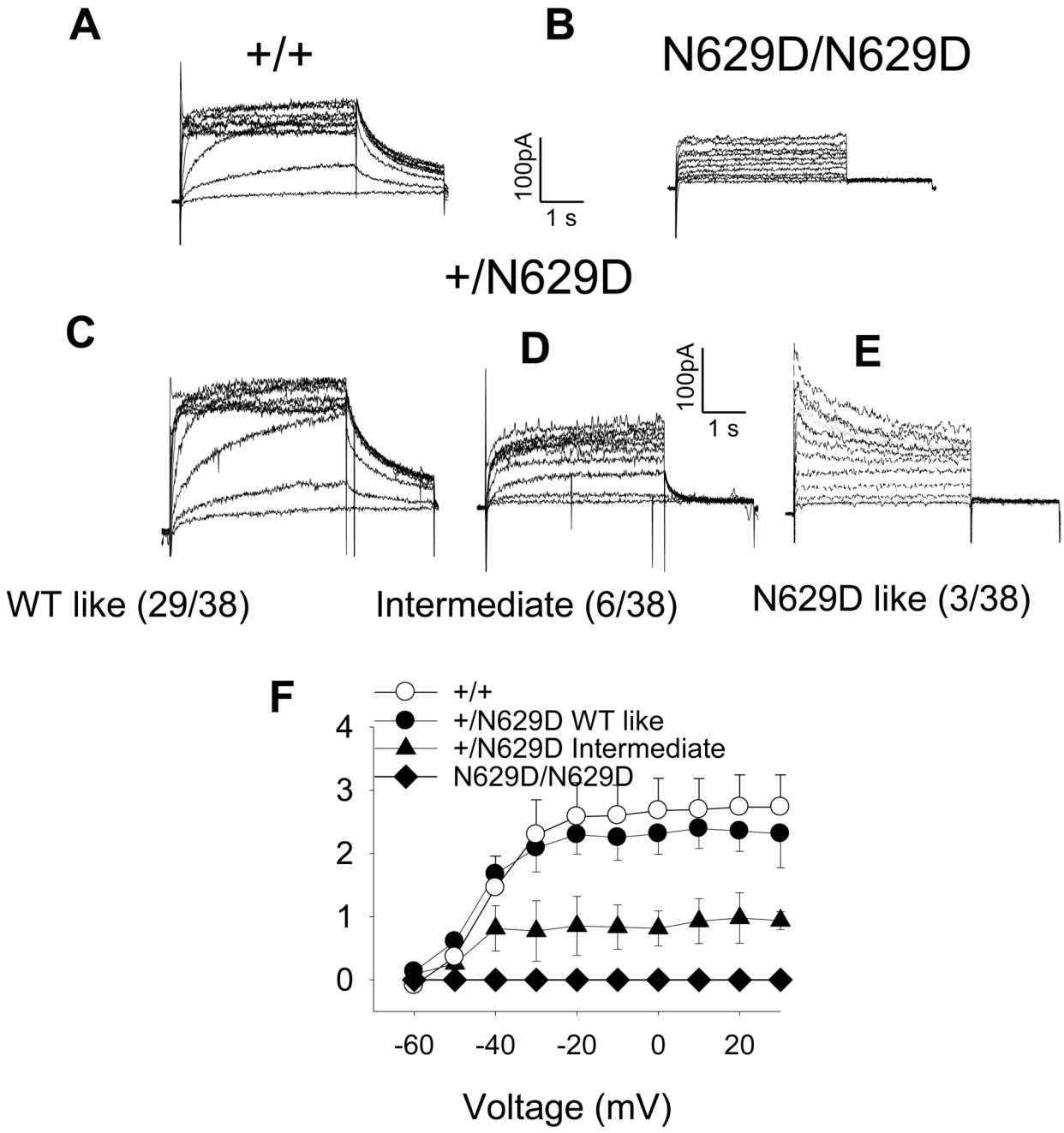

Figure 2. Representative I_{Kr} Records in +/+ versus homozygous and heterozygous N629D myocytes

Panel A shows representative examples of I_{Kr} recorded in E9.5 myocytes from +/+, Panel B N629D/N629D myocytes and Panels C, D and E +/N629D myocytes. In N629D/N629D embryos, the myocytes manifest no I_{Kr} tail-current. Most +/N629D heterozygous myocytes manifest a wild type-like I_{Kr} whereas the minority of cells show an N629D "intermediate" and N629D/N629D like phenotype. The numbers in the brackets show the number of cells which showed the various phenotypes in the +/N629D embryos. The mean current-voltage relationships are shown in Panel F. Data are significant ($P<0.001$) comparing WT to N629D/N629D and comparing WT to +/N629D cells showing an intermediate phenotype. The +/N629D cells with a wild type-like phenotype are not different compared to +/+. The mean tail-

current data for heterozygotes, manifesting an N629D-like phenotype are not show in Panel F, because they overlap with the N629D/N629D cells.

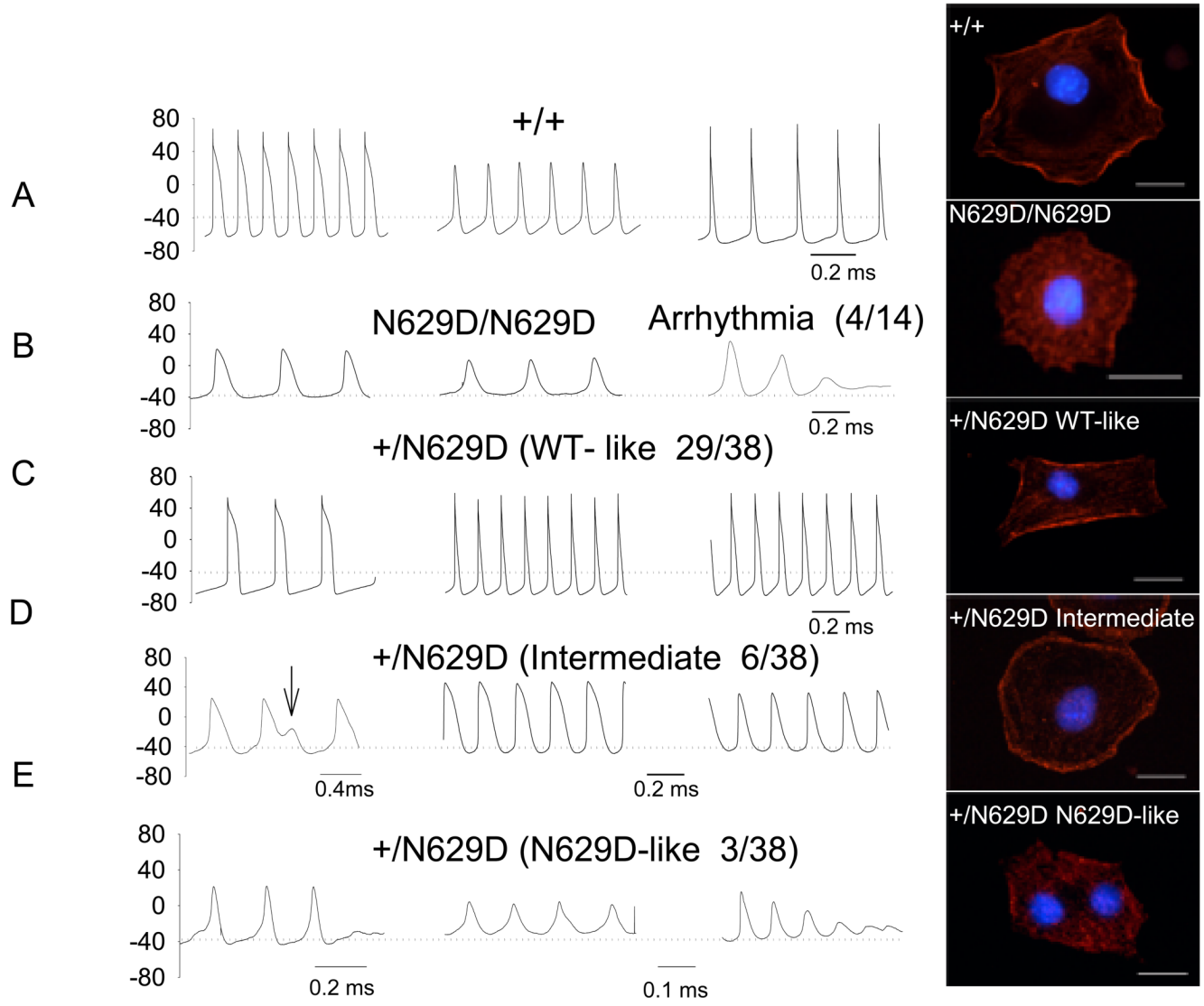

Figure 3. Representative action potentials recorded in +/+; homozygous and heterozygous N629D

For each and every cell, the I_{Kr} phenotype is evaluated in voltage-clamp mode was followed by recording the paired action potentials in current-clamp mode. Action potentials from +/+ myocytes manifest a spectrum of action potential durations and resting potential (Panel A) some with features of sinus node- like cells, some with features like atrial-like action potentials. In Panel B action potentials from N629D/N629D mice show homogeneous features: extreme depolarization, prolonged APD and failure to repolarize with oscillatory triggered arrhythmias. Action potentials recorded in heterozygous +/ N629D are related to the paired I_{Kr} phenotype : the action potentials associated with a WT-like I_{Kr} in Panel C and intermediate I_{Kr} phenotype in Panel D and N629D/N629D-like in Panel E. Heterozygous +/N629D WT- like myocytes have action potential features indistinguishable from +/+. Action potentials from +/N629D embryo hearts with an intermediate I_{Kr} phenotype show depolarization and prolonged APD, Arrowhead indicates EAD. Action potentials from +/N629D embryo hearts with N629D phenotype show similar pattern of N629D/N629D embryo hearts. The numbers with in the brackets show the number of cells which showed the various phenotypes in the +/N629D embryos.

Representative examples of the cellular distribution of the mERG proteins were evaluated in isolated cardiac myocytes and shown in the right hand column. The +/+ protein is dominantly expressed in the plasma-lemma whereas the N629D/N629D protein is dominantly expressed intracellularly (see text). A spectrum of patterns of protein expression are observed in the +/N629D heterozygous myocytes. The majority of cells (108/133) manifest a distribution pattern similar to WT. A minority of cells (14/133) have a distribution virtually identical to N629D/N629D. Another group of cells have a phenotype intermediate between WT and N629D/N629D. In these cells, the protein is distributed in a peri- or sub-plasma-lemmal location but the protein is expressed as punctuate dots, rather than the linear sheaths of protein seen in WT. The bars indicate 20 μM.

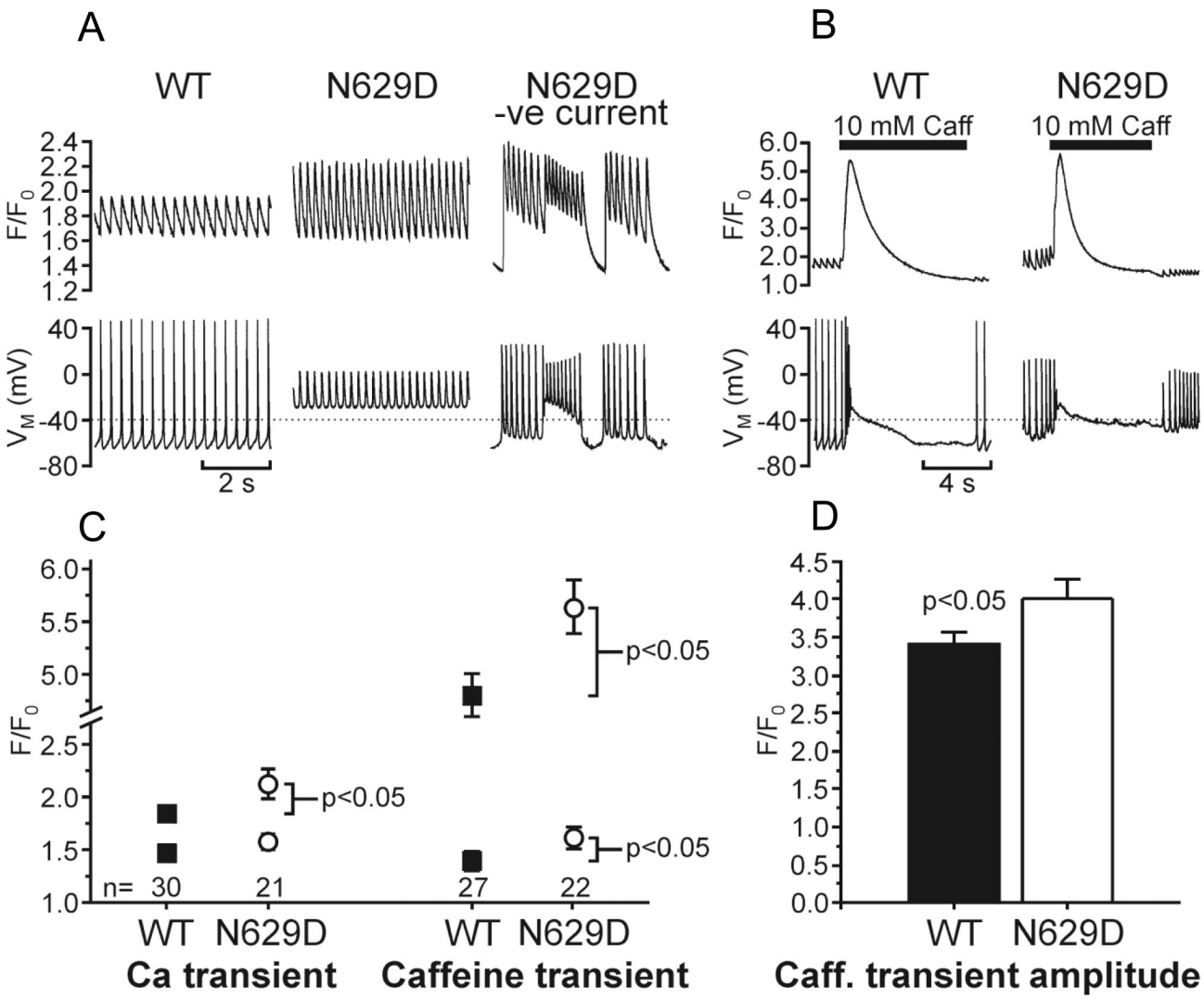

Figure 4. Intracellular calcium signals in voltage-clamped wild type (WT) and N629D/N629D E9.5 myocytes

A, B: Representative tracings. Upper panels show calcium signal (F/F_0), lower panels show membrane potential (V_M). In **A**, the WT cell displays spontaneous action potentials with corresponding calcium transients. The N629D cell is depolarized (resting membrane potential = −30 mV) and shows rapid oscillatory potentials and elevated peak [Ca^{2+}]. When its resting membrane potential is lowered to −65 mV by injecting negative current it exhibits abnormal action potentials with prominent early afterdepolarizations. **B:** Ca transients in response to rapid application of 10 mM caffeine. **C, D:** Summary data. Mean ± SEM is shown for Ca transients and caffeine-induced transients, with n (cells) indicated. Number of animals was 7 WT, 6 N629D. Statistically significant differences are shown. Error bars are omitted when smaller than symbols.

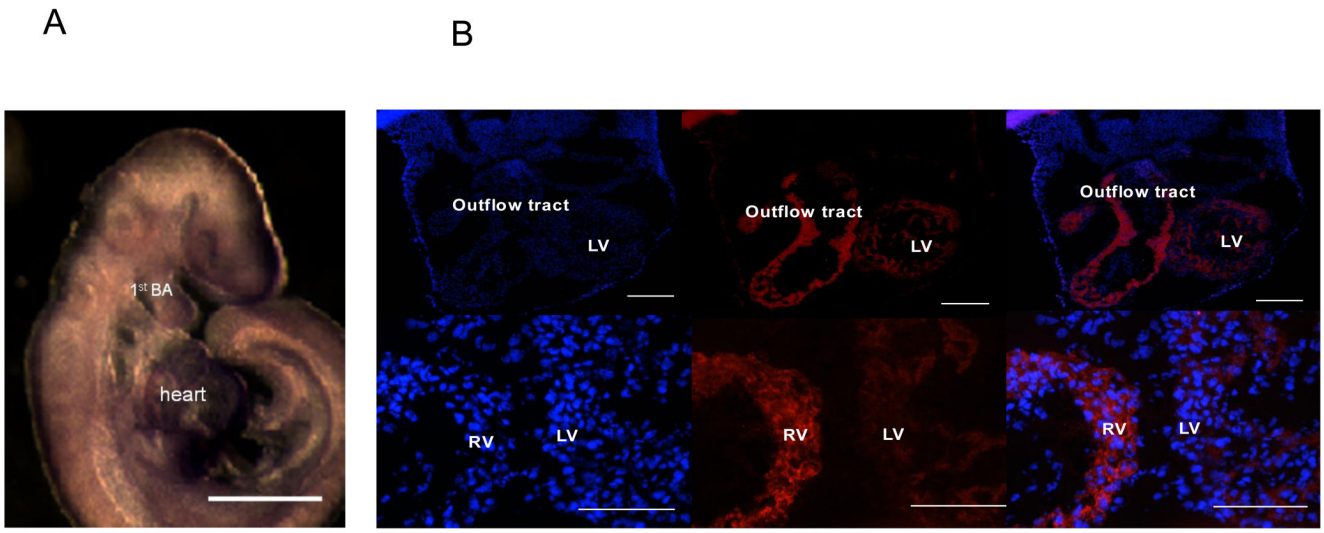

Figure 5. Spatial distribution of mERG protein expression in +/+ Embryos

Panel A shows *in situ* hybrization of mERG expression at E9.5. mERG is extensively expressed in the cranial-fascial region, the first branchial arch, and the heart. The bar indicates 200 μM. Panel B: Overall mERG protein expression is compared in the right ventricle and outflow tract to that observed in the left ventricle in the +/+ at E10.5 embryo heart. Panels B show the Dapi staining on the left mERG antibody staining in the middle and merged Dapi with mERG antibody staining in the right hand panel. Note that the scale bars differ in the top and bottom rows. Within the same section, expression of mERG is consistently more in the right ventricle and outflow tract compared to the left ventricle. This is not due to a difference in overall cell number as seen by the DAPI staining. RV indicates right ventricle, LV indicates left ventricle. Panel A bar indicates 200 μM and panel B indicates 100 μM.

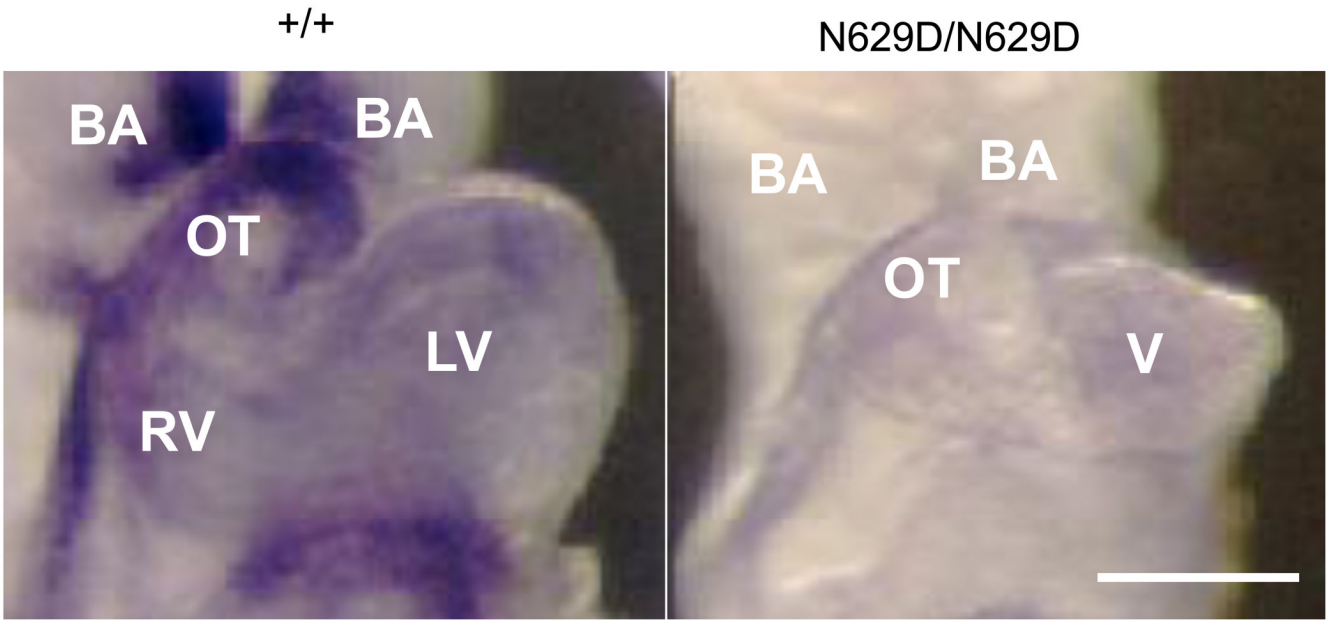

Figure 6. Representative examples of Hand 2 expression

In situ hybridizations are shown for +/+ (left) versus N629D/N629D embryos (right) at E9.5. Substantial *Hand2* expression is observed in the branchial arches (BA), outflow tract (OT), right ventricle (RV), with less expression in the left ventricle (LV). *Hand2* expression is downregulated in N629D/N629D embryos in these similar locations (right Panel). Bar indicate 200 μM.

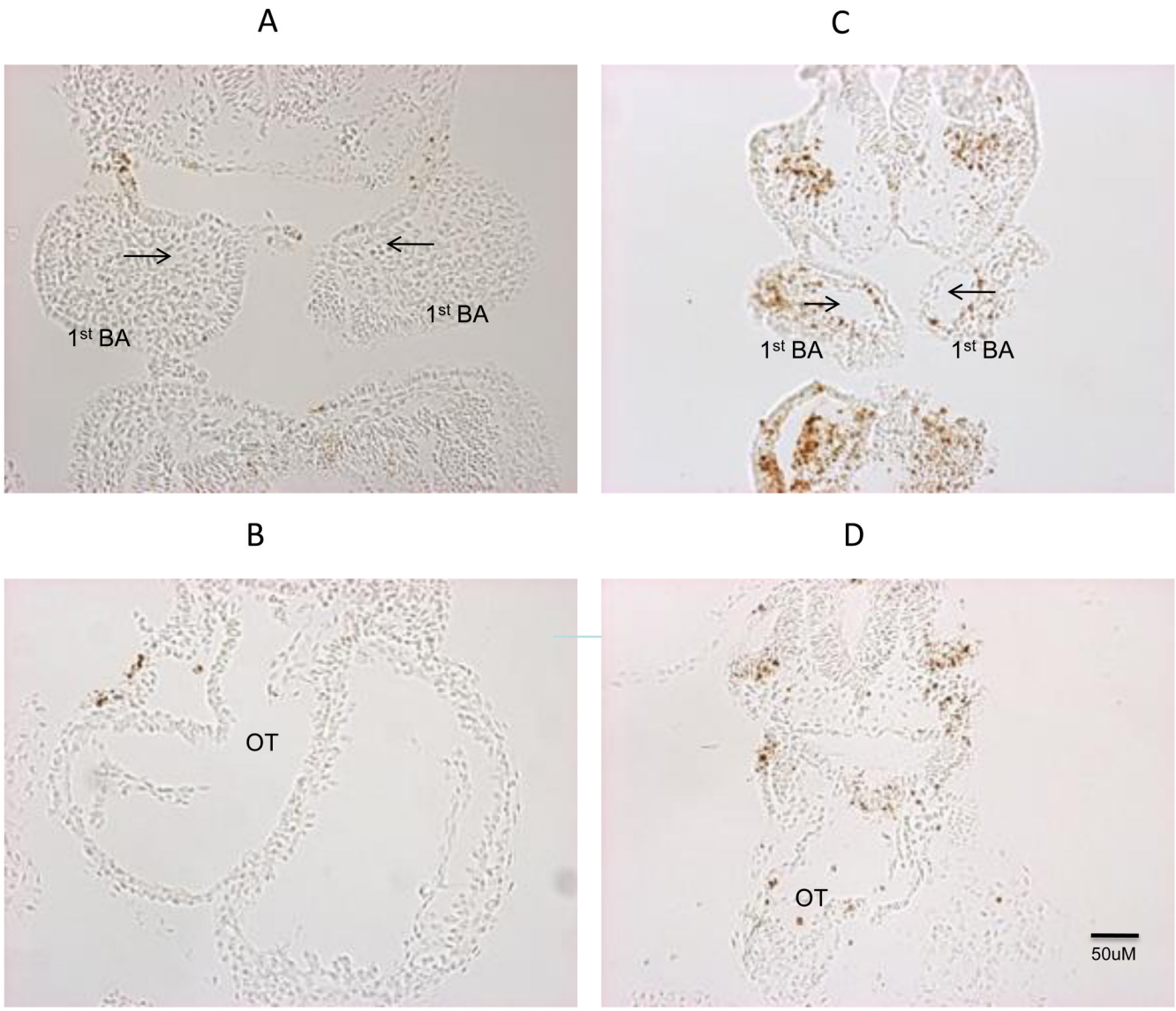

Figure 7. TUNEL assay for apoptosis

Cross sections through the first branchial arch shows robust TUNEL positive cells in the cranio-facial regions in N629D/N629D E9.5 embryos (Panel C and D) is compared to +/+ embryos (Panel A and B). The arrow indicates the first branchial arch artery. Cross sections through the heart show TUNEL positive cells sporadically in the N629D/N629D heart (bottom right panel). Apoptotic cells in the +/+ hearts were more rarely seen (bottom left panel).